PERIODICITIES OF SOLAR IRRADIANCE AND SOLAR ACTIVITY INDICES, I

JUDIT PAP

CIRES, University of Colorado/NOAA, Campus Box 216, Boulder, CO 80309, U.S.A.

W. KENT TOBISKA

Space Sciences Laboratory, University of California, Berkeley, CA 94720, U.S.A.

and

S. DAVID BOUWER

CIRES, University of Colorado/NOAA, Campus Box 216, Boulder, CO 80309, U.S.A.

(Received 21 March, 1990)

Abstract. Using a standard FFT time series analysis, our results show an 8-11 months periodicity in the solar total and UV irradiances, 10.7 cm radio flux, Ca–K plage index, and sunspot blocking function. The physical origin of this period is not known, but the evidence in the results exclude the possibility that the observed period is a harmonic due to the FFT transform or detrending. Periods at 150–157 and 51 days are found in those solar data which are related to strong magnetic fields. The 51-day period is the dominant period in the projected areas of developing complex sunspot groups, but it is missing from the old decaying sunspot areas. This evidence suggests that the 51-day period is related to the emergence of new magnetic fields. A strong 13.5-day period is found in the total irradiance and projected areas of developing complex groups. This confirms those results (e.g., Donnelly *et al.*, 1983, 1984; Bai, 1987, 1989) which show that 'active centers' are located 180 deg apart from each other.

Our study also shows that the modulation of various solar data due to the 27-day solar rotation is more pronounced during the declining portion of solar cycle than during the rising portion. This arises from that the active regions and their magnetic fields are better organized and more long-lived during the maximum and declining portion of solar cycle than during its rising portion.

1. Introduction

Study of periodicities in solar observational data, both ground-based and satellite observations, has long been of high interest. Existence of a long-term cycle about 11-year and short-term 27–28 days periods have been well established in numerous solar indices. These periods are related to the solar magnetic activity and to the modulation of solar features due to the solar rotation, respectively. A search for additional possible periodicities in solar data is essential, since any absolute detection of periodicity in active phenomena would have fundamental significance for our understanding of solar activity. Furthermore, solar irradiance is the main driver for the energy budget of Earth's atmosphere, thus these investigations may improve our understanding of the solar-terrestrial relationships.

Several papers have recently been published using various forms of time series analysis. The 27–28 days period in relative sunspot number, 10.7 cm radio flux data, solar ultraviolet irradiance and geomagnetic indices has been reported by several

Solar Physics **129:** 165–189, 1990.

authors (e.g., Simon, 1982; Donnelly, Heath, and Lean, 1982; Donnelly *et al.*, 1983, 1984; Rottman, 1983; Rottman and London, 1984; Simon *et al.*, 1987; Lean and Brueckner, 1988; Tobiska and Bouwer, 1989; Barth, Tobiska, and Rottman, 1990). However, it was surprising that in the high precision total solar irradiance, measured by the SMM/ACRIM radiometer, the 27–28 days periodicity was missing and the main period was at 23.5-day in 1980, the year of solar maximum (Willson, 1982; Frohlich, 1984; Pap, 1985). It has been pointed out that during the solar maximum the main period of projected areas of young developing sunspot groups is also at 23.5-day, while the old sunspots show the 27-day solar rotation (Pap, 1985, 1986; Frohlich and Pap, 1989). Besides the rotational period, a prominent period has been found at 13.5 days in the ultraviolet spectral bands but it has not been shown in the 10.7 cm radio flux (Donnelly, Heath, and Lean, 1982; Donnelly *et al.*, 1983).

A summary paper has been published by Lean and Brueckner (1988) on the intermediate solar variability. This paper suggests that the 155-day periodicity is not simply a feature of flare activity, in which it has been found first by Rieger *et al.* (1984), but it may be associated with those solar regions where strong magnetic fields are concentrated. There is some evidence for a period around 300-day, too (e.g., Delarche, Laclare, and Sadsaoud, 1985; London, Pap, and Rottman, 1989; Simon, 1989; Lean and Brueckner, 1988) in several data sets. However, the real physical origin of these periods has been doubted (Hudson, 1987, 1989), partly because in some cases the investigated data sets are not long enough to get any statistically significant result and these long

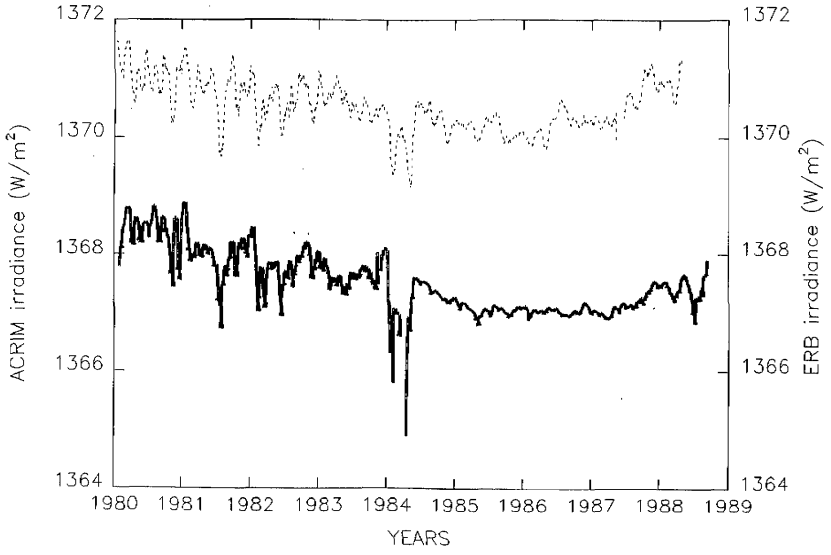

Fig. 1. 27-day running means of the SMM/ACRIM (heavy line) and Nimbus-7/ERB total irradiance data are presented. The ACRIM data refers to the time interval of February 1980 to September 1988. The ERB data refers to the time interval of January 1980 to May 1988.

periods may originate from the computational techniques used (e.g., from the way of detrending and smoothing the data). On the other hand, the existence of these periods depends strongly on the time interval that has been investigated. This rather would indicate a quasi-periodic or time-varying behavior, rather than a real cyclic behavior of various solar data. However, because of the importance of showing the real origin of the longer periodicities, further studies are required on this topic.

Our goal is to study the periodicities of different solar data and their time dependence as well, after removing the solar cycle-related long-term trends from the time series. Our paper is divided to two parts: in this first one (Paper I) we calculate the main periods of different data sets, such as solar total and ultraviolet irradiances, 10.7 cm radio flux, Ca–K plage index, projected sunspot areas, and sunspot blocking function. Since data sets for the 10.7 cm radio flux and for the sunspot blocking function cover 42 and

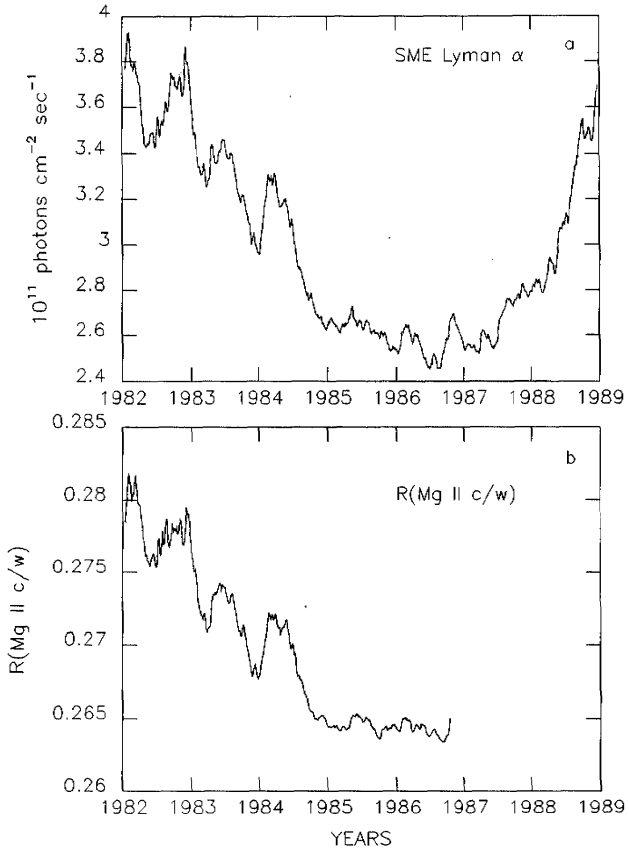

Fig. 2. (a) The 27-day running means of SME/Lα data for the time interval of January 1982 to December 1988. (b) The 27-day running means of the Nimbus-7/SBUV Mg II core-to-wing ratio, between January 1982 and December 1986.

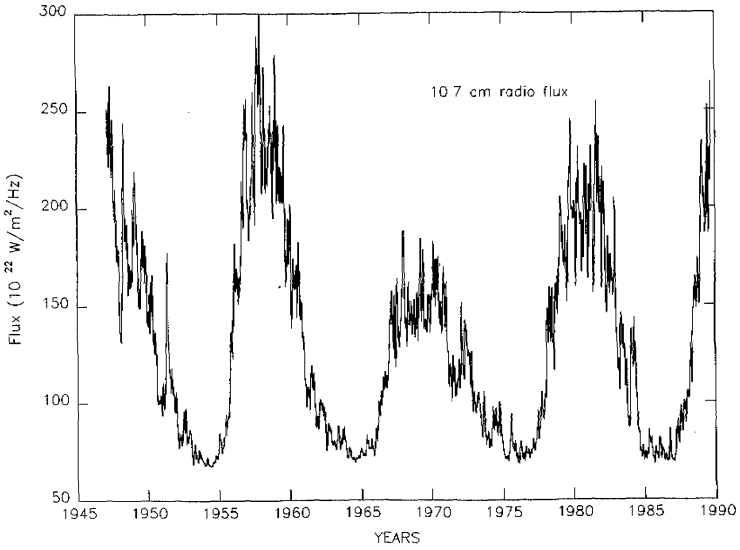

Fig. 3. 27-day running means of 10.7 cm radio flux are presented for the time interval of 1947 and 1989.

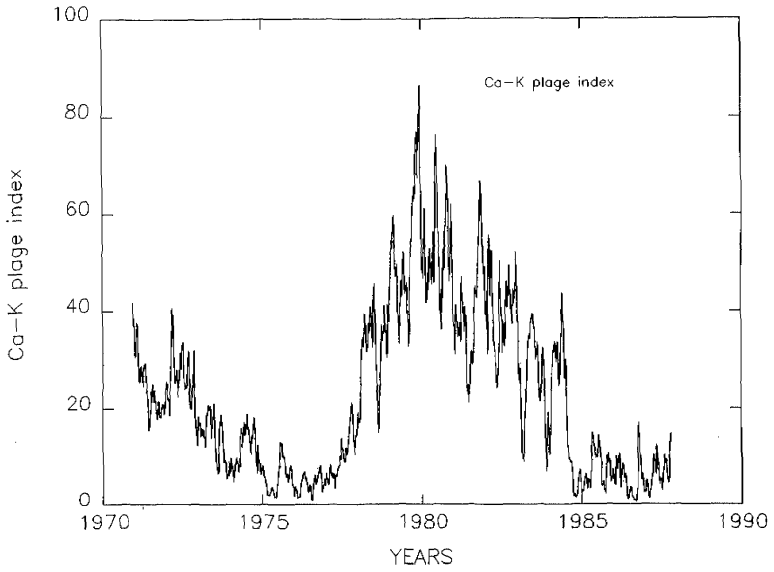

Fig. 4. 27-day running means of the Ca–K plage index are shown for the time interval of December 1970 to November 1987.

108 years, respectively, we can answer the question whether the longer periods around 300 or 155 days are statistically significant. There is also some indication that the amplitude of the period at 27-day solar rotation depends on the phase of solar cycle (e.g., Simon *et al.*, 1987). Therefore, in this paper we concentrate on the study of the 27–28 days period separately in the rising and declining portions of solar cycle. In the second part of our paper (Paper II) we will study the time dependence of the main periods shown in the above data sets, by using running power spectra with 25-day running windows. This method will establish how solar periodicities vary in frequency and amplitude over time.

2. Data Base

For over a decade that the solar irradiance has been observed continuously from space by several satellites. Measurements of total solar irradiance began in November 1978

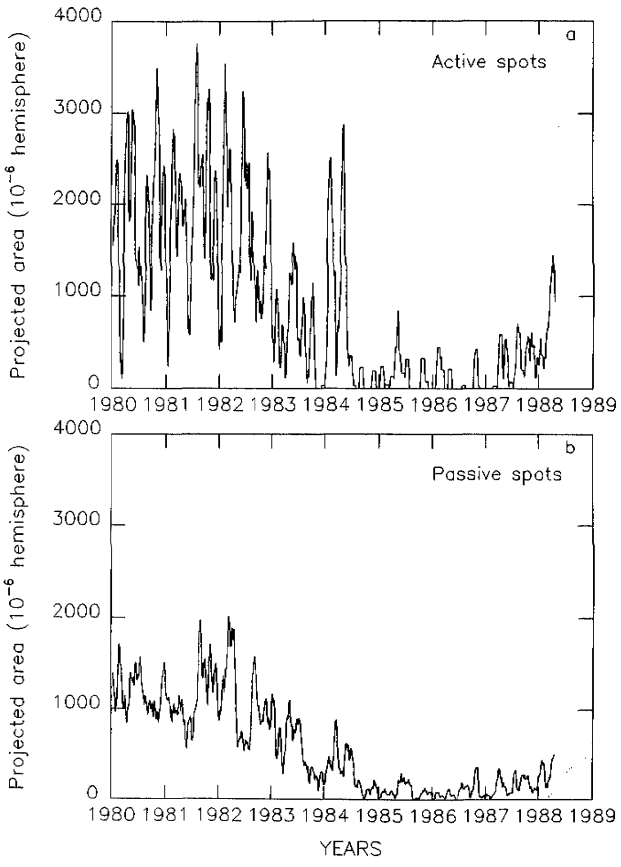

Fig. 5. (a) The 27-day running means of the projected areas of active sunspot groups. (b) The same for the passive spots. The time interval is between January 1980 and May 1988 in both cases.

on board Nimbus-7 satellite by the ERB active cavity radiometer (Hickey *et al.*, 1980, 1982). The high precision irradiance observations of the ACRIM radiometer on the Solar Maximum Mission satellite started in February 1980 (Willson *et al.*, 1981), when the measuring precision was so high ($\pm 0.002\%$) that every observed event had a solar, rather than an instrumental origin (Willson, 1984). In December 1980, when the SMM satellite was placed into the so-called 'spin-mode', the measuring precision of ACRIM radiometer failed by about a factor of 5 (from 0.002% to 0.01%). The SMM was repaired in May 1984 during a Shuttle Mission, and since that time the ACRIM data has regained the original high precision. The ERB experiment is still functioning as of this time and there are projections that this measurement mission could continue until 1991 (Hickey and Alton, 1984). The operation of the SMM/ACRIM instrument was ended in November 1989 (Willson, 1989). The ERB measurements, used for this study, cover the time interval of November 18, 1978 to April 30, 1988. The ACRIM data set, containing both the high precision data (between February and December 1980 and after May 1984) and spin-mode data (between December 1980 and May 1984), is used in this study for the time interval of February 14, 1980 to September 30, 1988.

Extensive measurements of the solar ultraviolet irradiance have been made by the Solar Backscatter Ultraviolet (SBUV) experiment on the Nimbus-7 satellite in the 160–400 nm spectral band since November 1978 (Heath, 1980) and by the solar spectrometer on the Solar Mesosphere Explorer (SME) satellite in the 120–305 nm range starting in October 1981 (Rottman *et al.*, 1982) and ending April, 1989 (Barth,

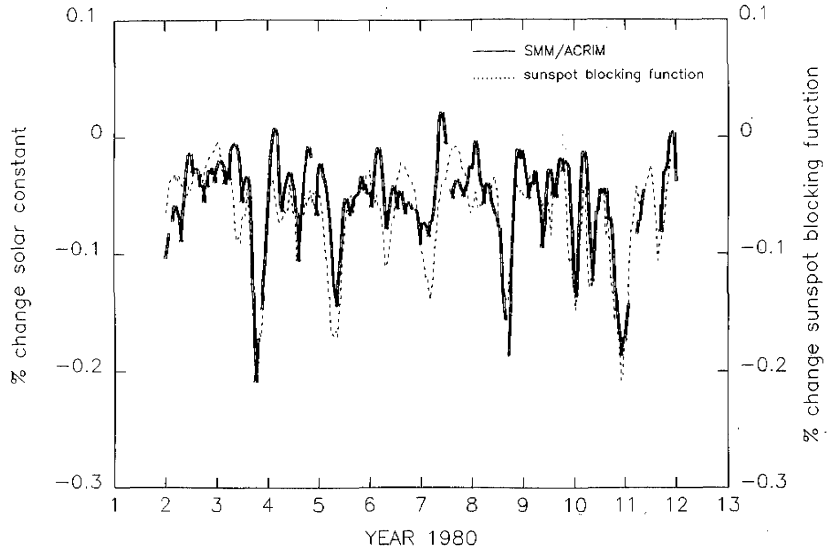

Fig. 6. Heavy line shows the percentage variation of the daily values of total irradiance measured by the SMM/ACRIM radiometer. Percentage variation of sunspot blocking function is given by the dashed line. Both curves refer for the time interval of February 1980 to December 1980.

Tobiska, and Rottman, 1990). Although the SBUV experiment suffers from a significant degradation in its diffuser reflectivity, the ratio of the irradiance in the core of the Mg 280 nm line to the irradiance at neighboring continuum wavelengths can be used as an index (Mg II h and k core-to-wing ratio) of solar variation (Heath and Schlesinger, 1986). Besides the Mg II (c/w) index, SME Lα (121.6 nm) data is used for investigating the UV irradiance variability. The SME Lα alpha data were calibrated by rocket flights, corrected for instrumental drift and degradation, adjusted to 1 AU, and linearly interpolated for days of missing data (London, Bjarnason, and Rottman, 1984). The long-term variability of Lα over the 11-year solar cycle is approximately a factor of 2, which exceeds the measuring uncertainty of the SME spectrometer, that is evaluated $\pm 2\%$ per year (Rottman, 1988).

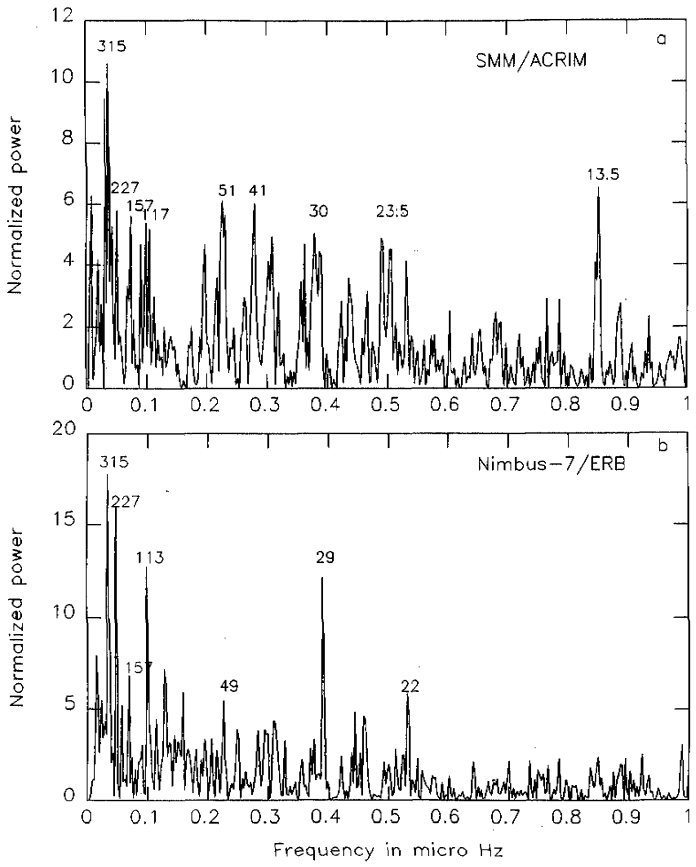

Fig. 7. Power spectra of the ACRIM and ERB total irradiance data are presented in Figure 7(a) and 7(b), respectively. The power is plotted in the 0–1 μHz (11.5-days) frequency range. The time interval of spectral analysis is from February 1980 to September 1988 for the ACRIM data and from November 1978 to May 1988 for the ERB data.

Daily values of 10.7 cm radio flux, Ca–K plage index and projected areas of sunspot groups are used as indices of solar activity. 10.7 cm radio flux (denoted here as $F10.7$) has been measured daily in Ottawa since 1947 and is reported on a regular basis adjusted to 1 AU. The daily $F10.7$ values are published in the NOAA/World Data Center (NOAA/WDC) *Solar Geophysical Data* catalogue. The Ca–K plage index data set contains three sources of data: (1) observations of plages in Ca–K line from December 1970 to September 1979 at the McMath Observatory, (2) from October 1979 to August 1982 at the Mt. Wilson Observatory, and (3) between September 1982 and November 1987 at the CALTECH/Big Bear Solar Observatory. The plage index is provided for this study by the NOAA/WDC. Projected areas of sunspots are published in the *Solar Geophysical Data* (SGD) and *Solnechnye Dannye* (SD) catalogues. Data sets for projected areas of 'active' and 'passive' sunspot groups were created by using informa-

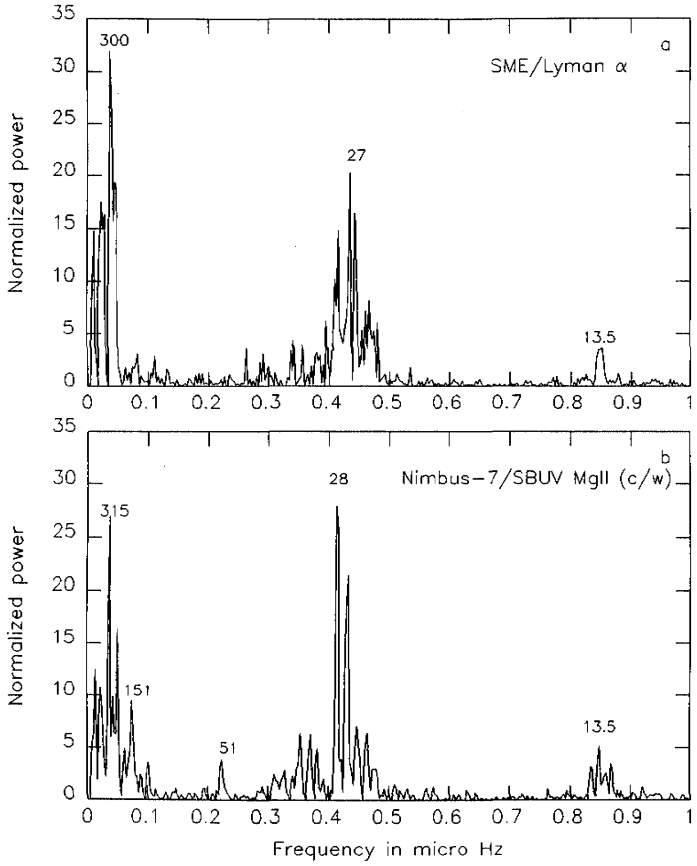

Fig. 8. Power spectra of SME/Lα and SBUV/Mg II core-to-wing ratio are presented in Figure 8(a) and 8(b). The time interval of analysis is between January 1982 and December 1988 for the SME Lα data, and November 1978–December 1986 for the Nimbus-7 SBUV Mg II c/w ratio.

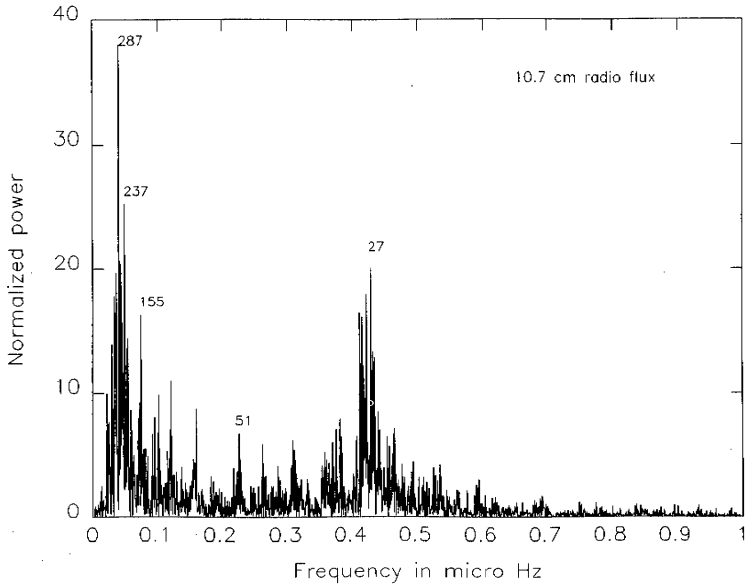

Fig. 9. Power spectrum of the 10.7 cm radio flux is presented for the time interval of 1947 to 1989.

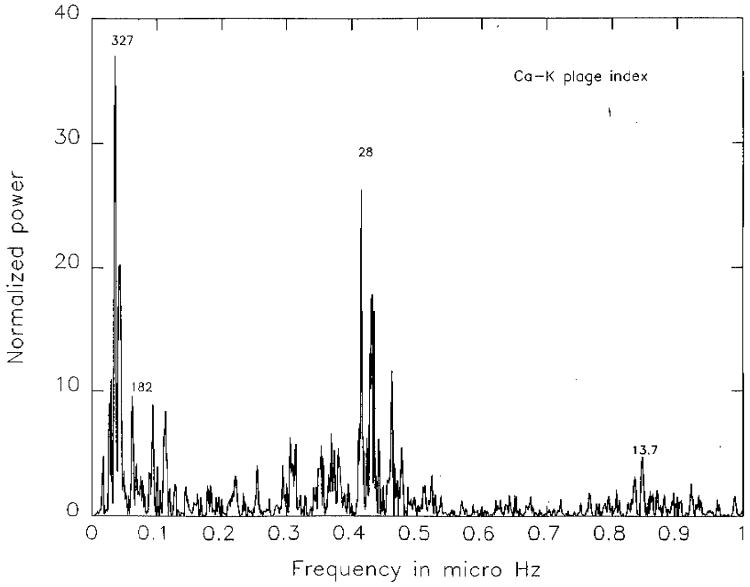

Fig. 10. Power spectrum of Ca–K plage index is given for the time interval of December 1970 to December 1987.

tion on age and magnetic structure of sunspots from SGD, and daily area of sunspots from SD. 'Active' sunspot groups have been defined as newly formed and growing complex groups with gamma and/or delta magnetic configurations. 'Passive' groups are the old simple groups with alpha or beta magnetic configurations. More details on this sunspot-classification are given by Pap (1985, 1986). Note that the active sunspot groups are usually Dkc, Ekc, or Fkc groups in the McIntosh classification system (e.g., McIntosh, 1981).

The sunspot blocking function used in this study has been created by Hoyt and Eddy (1982). This function relates observed sunspot areas and their contrast to a net effect on the radiative output of the observed solar hemisphere and it is corrected for the photospheric limb darkening. Daily values of sunspot blocking function were provided by the NOAA/WDC for a 108-year long time interval between 1874 and 1982.

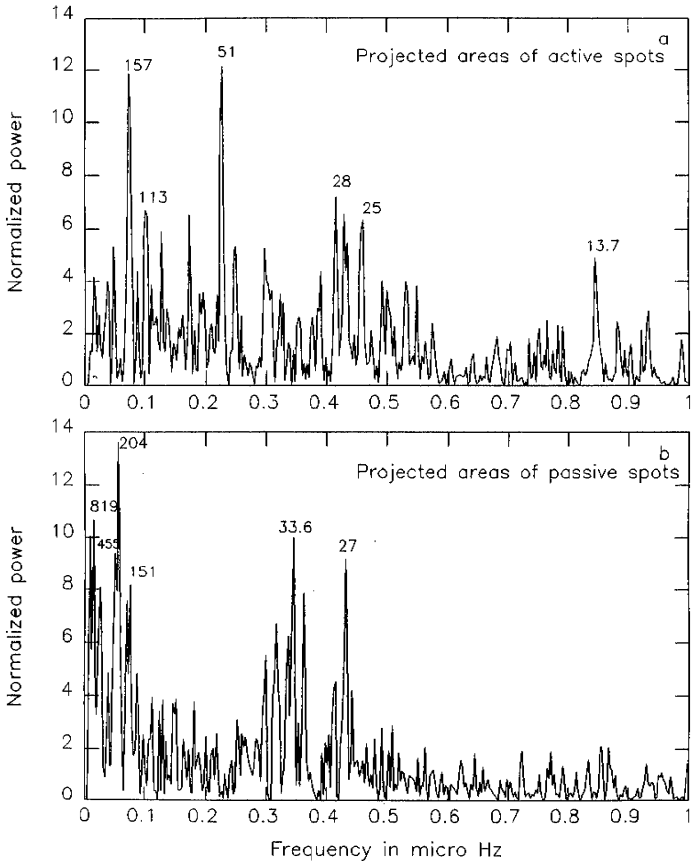

Fig. 11. Power spectra of projected areas of active and passive spots are given in Figure 11(a) and 11(b), respectively. The time interval is between January 1980 and May 1988.

3. Variability of Solar Irradiance and Activity Indices

The 27-day running means of the Nimbus-7/ERB and SMM/ACRIM total irradiance data are reproduced in Figure 1. Both the ERB and ACRIM data sets show a long-term variability related to the solar cycle. The total irradiance decreases continuously from the end of 1978 until mid-1985, whose amount is approximately 0.1% (Willson *et al.*, 1986). As can be seen from Figure 1, the ERB observations show a larger variability in the minimum time than the ACRIM ones, that is probably due to the larger measuring uncertainty in the ERB data set (Willson, 1989). In addition, the ERB data shows a different upward trend, that is a stronger increase of the total irradiance which has started almost a year before than it is shown by the ACRIM data. The reason of this discrepancy is still being investigated. As can be seen from Figure 1, dips in the total irradiance, caused by sunspots (e.g., Willson *et al.*, 1981; Hudson *et al.*, 1982) generally correspond to each other.

Figures 2(a) and 2(b) show the 27-day running means of the SME Lα and Nimbus-7 SBUV Mg II (c/w) index, respectively. As can be seen, both the short- and long-term

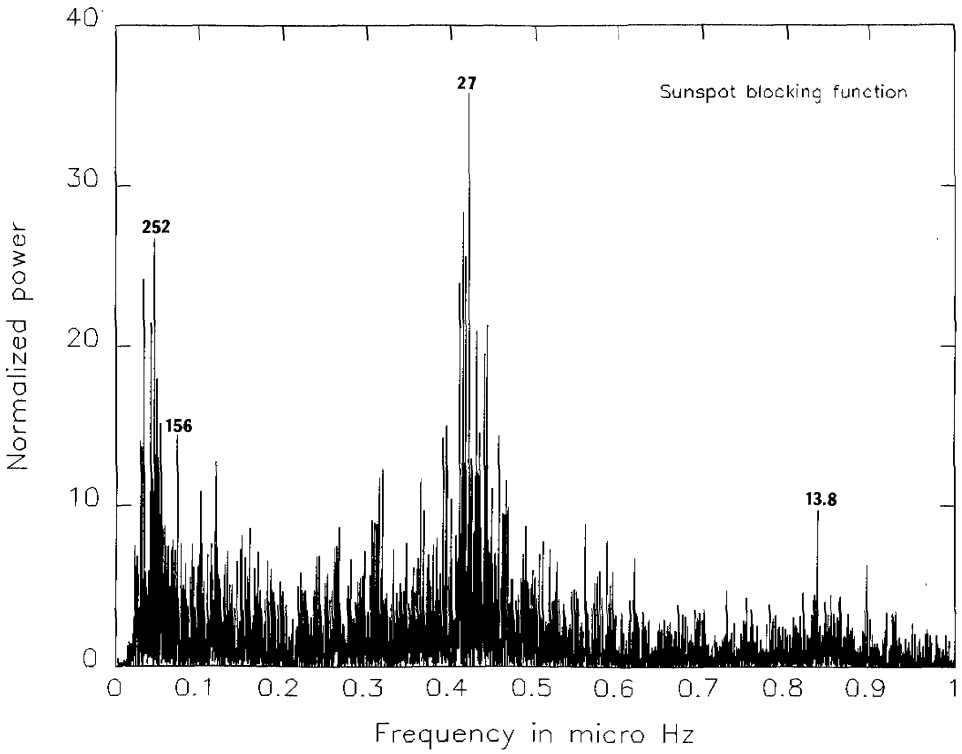

Fig. 12. Power spectrum of the 108-year long time series of sunspot blocking function is reproduced in Figure 12, between 1874 and 1982.

variabilities of the two data sets fit each other quite well (e.g., Tobiska and Bouwer, 1989). The correlation coefficient is 0.97 for their daily values and 0.98 for the 27-day running means. This gives a confidence that the variations are indeed of solar, rather than instrumental, origin. The SME/Lα data tends to decrease continuously until mid-1986 (Donnelly, 1989; Barth, Tobiska, and Rottman, 1990; Pap, London, and Rottman, 1990), while SBUV Mg II (c/w) ratio shows rather a double minimum: a primary one in mid-1985 and a secondary minimum in mid-1986.

Figure 3 gives the 27-day running means of $F10.7$ between 1947 and 1989. This curve represents well the strong 11-year modulation due to the solar magnetic activity (see also Tapping, 1987). Ca–K plage index (27-day running means) is shown in Figure 4, between 1970 and 1987, that also demonstrates a strong variation over the solar cycle.

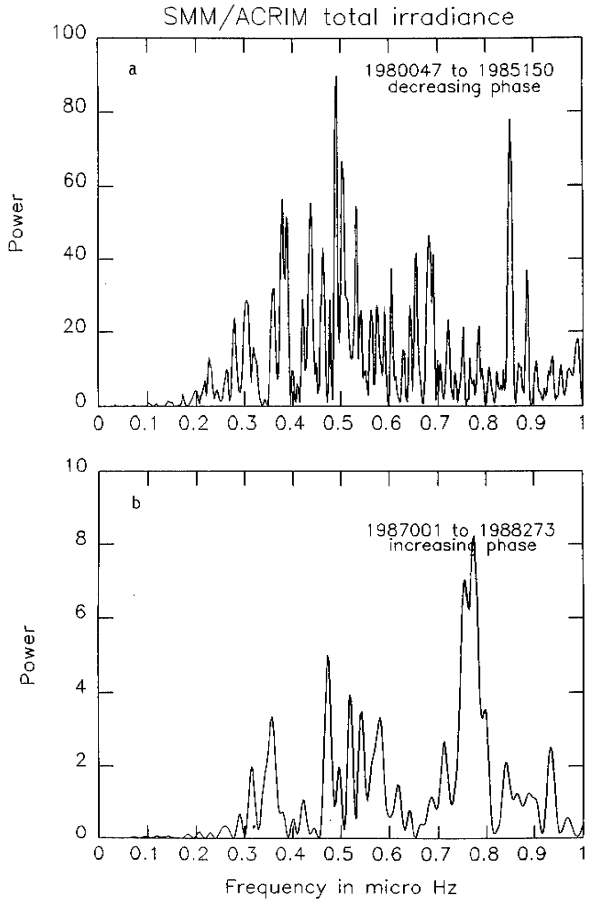

Fig. 13. (a) The power spectrum of ACRIM irradiance data for the decreasing phase of cycle 21. (b) The power spectrum for the rising portion of cycle 22.

27-day running means of projected areas of active and passive sunspot groups are shown in Figures 5(a) and 5(b), respectively. As can be seen, the area of active sunspot groups is larger than that of the old decaying spots, and both spot areas decrease towards the time of solar minimum.

As an example, Figure 6 shows the percentage variation of daily values of the SMM/ACRIM irradiance data (heavy line) and of the sunspot blocking function (dashed line) for 1980, the year of solar maximum (see also Willson *et al.*, 1981; Hoyt and Eddy, 1982). The dips in the ACRIM data generally correspond to the dips in the sunspot blocking function which indicates that sunspots modify mainly the total irradiance on daily/weekly time-scale (e.g., Willson *et al.*, 1981; Hudson *et al.*, 1982). However, the amplitudes of the dips in the observed and calculated total irradiance

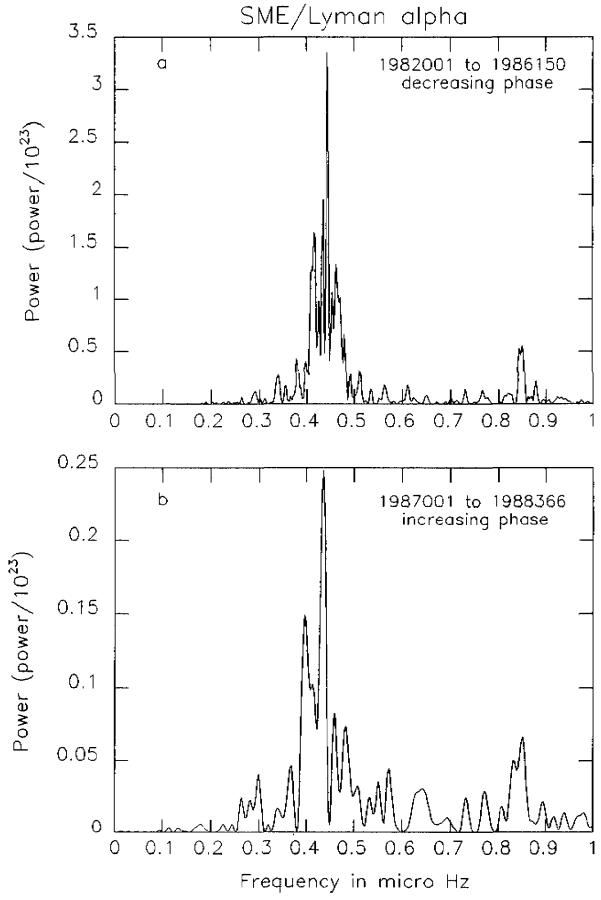

Fig. 14. (a) The power spectrum of SME/Lα data for the declining portion of cycle 21. (b) The same for the rising portion of solar cycle 22.

differ in some cases (see also Hoyt and Eddy, 1982). The correlation coefficient ($r = 0.79$) between the observed and calculated irradiance values also indicates that sunspots themselves can not explain all the irradiance variabilities (see also Willson *et al.*, 1981; Willson, 1982; Willson and Hudson, 1988). Note that several papers (e.g., Pap, 1985; 1986; Frohlich and Pap, 1989) showed that the sunspot-related irradiance dips are caused by young developing spots, while the old spots tend to increase the value of total irradiance. This indicates that the sunspot effect is overcompensated by the excess flux of faculae in the old active regions. This also suggests that the irradiance models may be improved by taking into account the evolutionary processes.

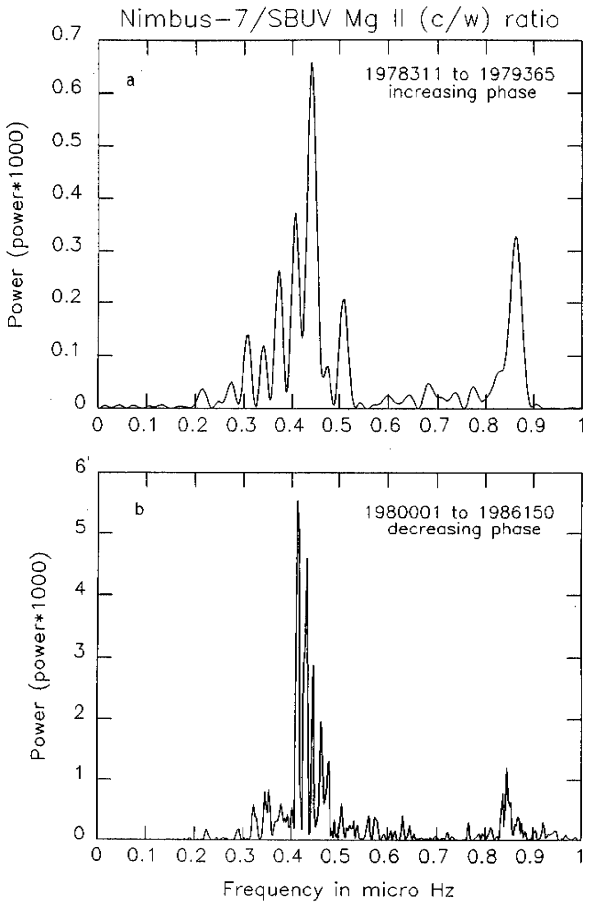

Fig. 15. Power spectra of Nimbus-7/SBUV Mg II c/w ratio are presented for the rising portion of cycle 21 (a) and for the declining portion of cycle 22 (b).

4. Time Series Analysis

4.1. METHOD

The frequency spectrum of all time series is calculated for frequencies up to 1.65 μHz (about 7 days) with a standard fast Fourier transform (FFT) technique. In order to

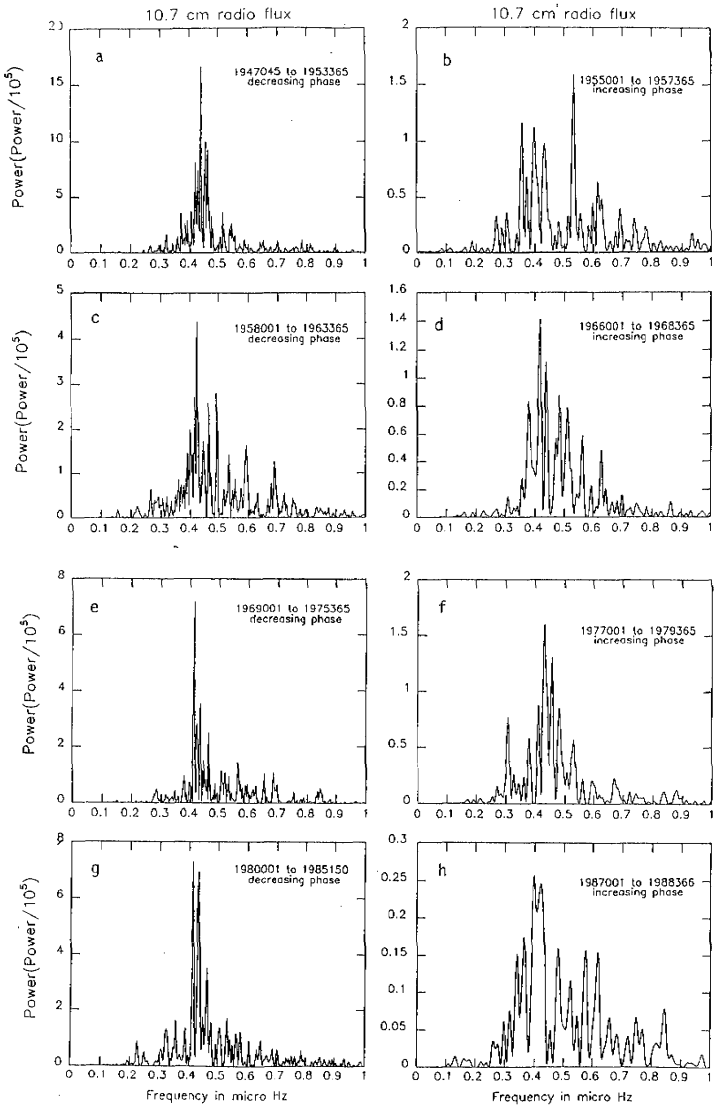

Fig. 16. Power spectra of the 10.7 cm radio flux are presented for the rising and declining portions of different solar cycles (from cycles 18 to 22). The time interval of period analysis is presented on each plot.

eliminate the solar cycle related long-term trends, 365-day running means of the data were subtracted from the daily values (e.g., Bath, 1974). When the data set does not cover a whole solar cycle, a 4th-degree polynomial fit is used for removing the long-term trend related to the 11-year solar cycle. The missing data in the time series has been replaced by the mean of the data sets. Table I gives the number of missing data for each data set. Before employing FFT on the time series, their overall mean had been subtracted from each observation (e.g., Chatfield, 1984). Normalization of the power density spectra has been made in such a way that the normalization factor is the average of the power densities in the 0–1.65 μHz frequency domain. The poser densities are averaged only up to frequency of 1.65 μHz since the solar origin of periods shorter than 7-day is not significant from the present time resolution of the data used in our study.

We also examine the periodicity of different solar data around the 27-day rotational period, separately for the rising and declining portions of solar cycle. For this purpose every periodicity longer than 27-day has been removed from the time series by means of a 27-day running mean (see also Bath, 1974; Chatfield, 1984). The 27-day averaged values have been subtracted from the original data values. The method for the FFT is

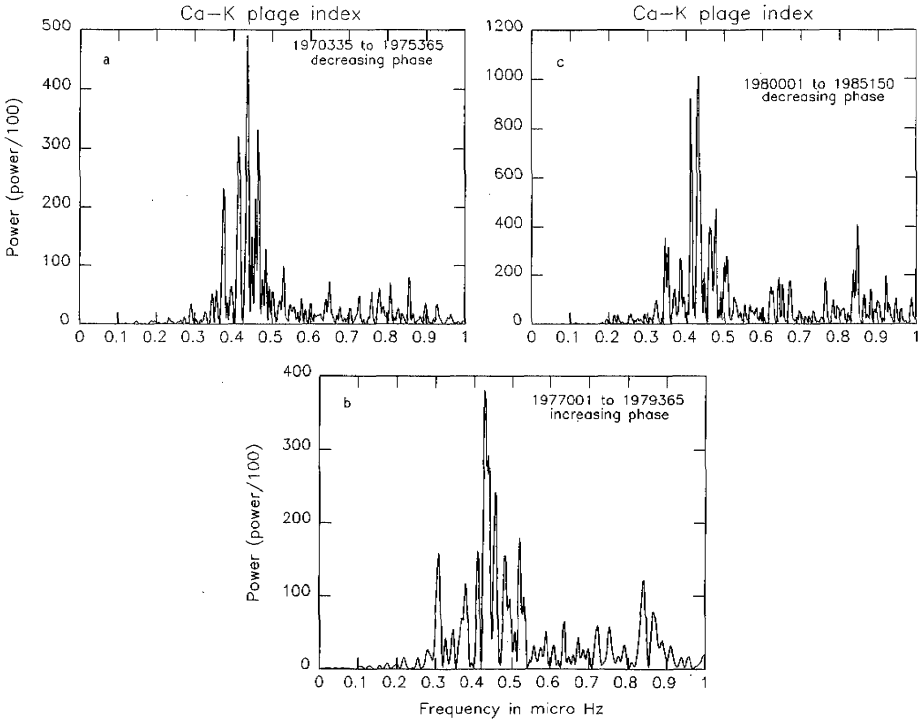

Fig. 17. Power spectra of Ca–K plage index are given, for the decreasing phase of cycle 20 (a), and for the increasing (b), and decreasing (c) phases of cycle 21.

TABLE I

Numbers of all data points and of missing data are listed for the investigated time series. Numbers of valid data in percentage are also given. In the column of time interval (yyyyxxx), the year (yyyy), and number of days (xxx) are given.

Time series	Time interval	Numbers of		
		All data	Missing data	Valid data (%)
SMM/ACRIM	1980047–1988273	3150	328	89
Nimbus-7/ERB	1978305–1988121	3469	563	83
SME Lα	1982001–1988366	2557	0	100
SBUV MG II	1978311–1986301	2913	839	71
F10.7 cm	1947045–1989170	15467	0	100
Plage index	1970335–1987308	6183	1391	77
Active spot	1980001–1988121	3043	5	99
Passive spot	1980001–1988121	3043	5	99
Sc function	1874001–1982365	39811	6487	83

the same as described above, except for that for this latter study the power densities have not been normalized.

4.2. Results of Time Series Analysis

4.2.1. *Solar Irradiances*

Periodicities of SMM/ACRIM data and Nimbus-7/ERB data have been investigated for the time intervals of February 1980 to September 1988, and November 1978 to May 1988, respectively. Power spectra of the above time series are given in Figures 7(a) and 7(b). The power densities are plotted in the 0–1 μHz (1 μHz is about 11.5-day) frequency domain with a resolution of 0.003 μHz. The main feature of Figures 7(a) and 7(b) is the lack of a period at 27-day in the total irradiance. In the ERB data the most dominant period is at 29-day (Hickey *et al.*, 1982) around the solar rotational period, and there is a smaller peak at 22-day. In the ACRIM data, around the solar rotation, there is a strong period at 23.5-day (see also Willson, 1982; Frohlich, 1984; Pap, 1985; Frohlich and Pap, 1989) and also a peak at 30-day. Additional periods are seen in both data sets around 50, 113, 157, 227, and 315 days. In the ACRIM time series strong periods are seen about 41 and 13.5 days which are missing from the ERB data set.

Power spectra of SME Lα and SBUV/Mg II (c/w) ratio are seen in Figures 8(a) and 8(b). As can be seen, for both data sets the main periods are around 300 (300-day for the SME Lα, 315-day for the SBUV Mg II (c/w) ratio), 27 and 13.5 days. There is a little evidence for periods at 151 and 51 days in the Mg II (c/w) ratio.

4.2.2. *Solar Activity Indices*

The power spectrum of F10.7 is presented in Figure 9, with a frequency resolution of 0.0007 μHz. The major period is at 287-day and peaks are seen around 330 and 237 days, too. Additional periods are found at 155-day, its amplitude is about half of

Additional periods at 113 and 13.7 days exist for the active spot areas which cannot be seen in the case of passive spots. The projected areas of passive spots have more power towards the shorter frequencies: the main period is at 204-day and additional periods are seen at 455 and 819 days which are missing from the spectrum of active spots.

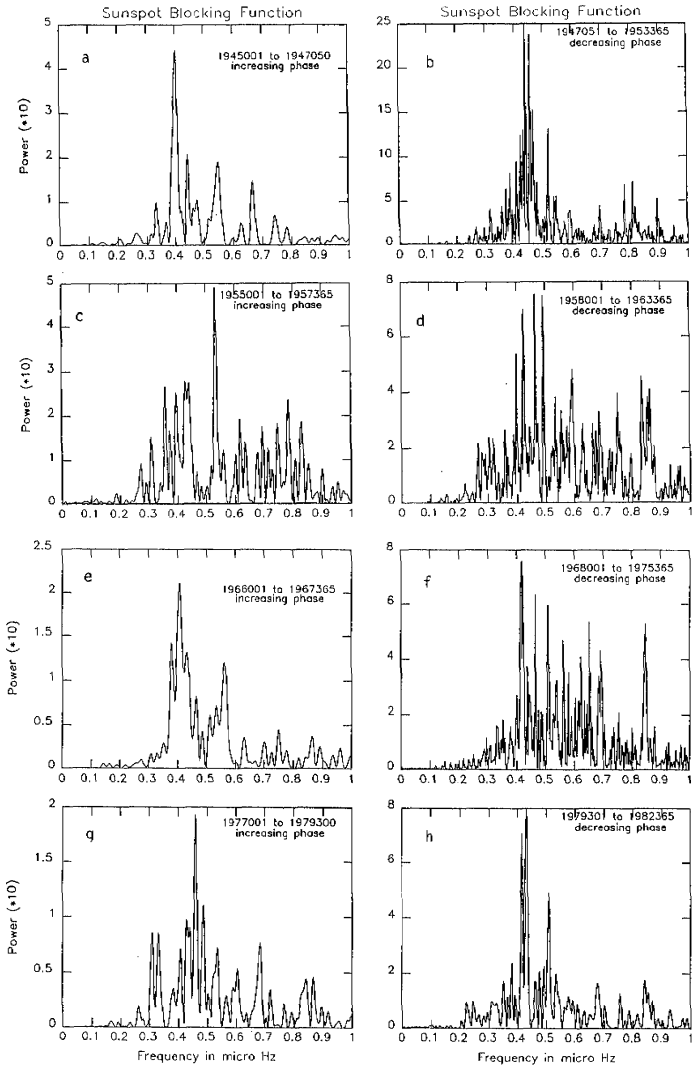

Fig. 19. Power spectra of sunspot blocking function are shown for the increasing and decreasing phases of different solar cycles, between 1945–1982. The time interval of period analysis is written on each plot.

4.2.3. *Sunspot Blocking Function*

Periodicities of sunspot blocking function have been investigated for a 108-year long interval of 1874–1982. This interval involves 11 solar cycles, cycles 11 through 21. For cyles 11 and 21 data exist only for a part of their descending phases. The time resolution for the frequency spectrum of sunspot blocking function is about 0.0004 μHz. Figure 12 shows the power spectrum of the sunspot blocking function for the time interval of 1874–1982. As can be seen, the main period is at 27.5 days, showing the strong modulation due to the solar rotation. A small, but still significant peak is seen at 13.8-day. At longer periods the main periodicity is at 252-day, but additional periods are seen also at 280 and 350 days as well. There is some evidence from this 108-year long data set for the existence of a period about 156 days (0.074 μHz).

4.3. The 27-day rotational periodicity

In this section we study the dependence of the periodicity due to the solar rotation on the phase of solar cycle. For this purpose, periodicities have been calculated separately for the descending and ascending phases of different solar cycles. Any periodicities, which are longer than 27 days have been removed from the data sets by means of a 27-day running mean (see Section 4.1). Each power spectrum is plotted in the 0–1 μHz frequency domain, with a resolution about 0.003 μHz.

Figures 13(a) and 13(b) show the power spectra of the SMM/ACRIM data for the declining portion of cycle 21 (1980–1985) and for the rising portion of cycle 22 (1987–1988), respectively. The same is seen in Figures 14(a) and 14(b) for the SME Lα data. Figures 15(a) and 15(b) give the power spectra for the SBUV/Mg II (c/w) ratio for the rising portion of cycle 21 (1978–1979) and declining portion of cycle 21 (1980–1986). Power spectra for $F10.7$ are given in Figures 16(a–h). The time intervals, for which the FFT has been employed, are written on each plot. Figures 17(a–c) show the 27-day periodicity in the power spectra of Ca-K plage index, for the declining phase of cycle 20 (1970–1975), rising portion of cycle 21 (1977–1979) and for the declining portion of cycle 21 (1980–1985).

Power spectra of projected sunspot areas are given in Figures 18(a) (active spots) and 18b (passive spots). Power spectra are calculated for the declining portion of cycle 21 (1980–1985) (upper panels) and the rising portion of cycle 22 (1987–1988) (lower panels). Figures 19(a–h) give the power spectra of sunspot blocking function for the increasing and decreasing phases of solar cycles 18–22. The time intervals for the FFT are seen on the plots. As can be seen from Figures 13–19, the amplitude of the power around the 27-day is systematically higher for the declining portions than for the rising ones, in each case of the investigated data sets. The result is the same for the sunspot blocking function for solar cycles 11–17, as can be seen from Table II (also Pap, 1989).

In order to compare the amplitudes (referring for the rising and declining portions of solar cycles) quantitatively we have calculated the ratio of power amplitudes in the following way. The amplitude of power around the solar rotation in the declining portion of the cycle is divided with the amplitude of power around the rotational period in the